

o-Quinone Methide as Alkylating Agent of Nitrogen, Oxygen, and Sulfur Nucleophiles. The Role of H-Bonding and Solvent Effects on the Reactivity through a DFT Computational Study

Cristiana Di Valentin, Mauro Freccero,* Riccardo Zanaletti, and Mirko Sarzi-Amadè

Contribution from the Dipartimento di Chimica Organica, Università di Pavia, V.le Taramelli 10, 27100 Pavia, Italy

Received February 19, 2001. Revised Manuscript Received June 11, 2001

Abstract: The reactivity of the alkylating agent *o*-quinone methide (*o*-QM) toward NH₃, H₂O, and H₂S, prototypes of nitrogen-, oxygen-, and sulfur-centered nucleophiles, has been studied by quantum chemical methods in the frame of DF theory (B3LYP) in reactions modeling its reactivity in water with biological nucleophiles. The computational analysis explores the reaction of NH₃, H₂O, and H₂S with *o*-QM, both free and H-bonded to a discrete water molecule, with the aim to rationalize the specific and general effect of the solvent on *o*-QM reactivity. Optimizations of stationary points were done at the B3LYP level using several basis sets [6-31G(d), 6-311+G(d,p), adding d and f functions to the S atom, 6-311+G(d,p),S(2df), and AUG-cc-pVTZ]. The activation energies calculated for the addition reactions were found to be reduced by the assistance of a water molecule, which makes easier the proton-transfer process in these alkylation reactions by at least 12.9, 10.5, and 6.0 kcal mol⁻¹ [at the B3LYP/AUG-cc-pVTZ//B3LYP/6-311+G(d,p) level], for ammonia, water, and hydrogen sulfide, respectively. A proper comparison of an uncatalyzed with a water-catalyzed reaction mechanism has been made on the basis of activation Gibbs free energies. In gas-phase alkylation of ammonia and water by *o*-QM, reactions assisted by an additional water molecule H-bonded to *o*-QM (water-catalyzed mechanism) are favored over their uncatalyzed counterparts by 5.6 and 4.0 kcal mol⁻¹ [at the B3LYP/6-311+G(d,p) level], respectively. In contrast, the hydrogen sulfide alkylation reaction in the gas phase shows a slight preference for a direct alkylation without water assistance, even though the free energy difference ($\Delta\Delta G^\ddagger$) between the two reaction mechanisms is very small (by 1.0 kcal mol⁻¹ at the B3LYP/6-311+G(d,p),S(2df) level of theory). The bulk solvent effect, evaluated by the C-PCM model, significantly modifies the relative importance of the uncatalyzed and water-assisted alkylation mechanism by *o*-QM in comparison to the case in the gas phase. Unexpectedly, the uncatalyzed mechanism becomes highly favored over the catalyzed one in the alkylation reaction of ammonia (by 7.0 kcal mol⁻¹) and hydrogen sulfide (by 4.0 kcal mol⁻¹). In contrast, activation induced by water complexation still plays an important role in the *o*-QM hydration reaction in water as solvent.

Introduction

Quinone methides (QMs) are interesting reactive intermediates because they can be involved in a large number of chemical and biological processes such as biosynthesis of lignin¹ and enzyme inhibition.^{2–7} Among hydrolase inhibitors,^{3–7} QMs have recently been used as covalent β -lactamase,⁵ phosphatase,^{4,6} and ribonuclease A⁷ inactivators. It has been suggested that quinone methide structures play a key role in the chemistry of several classes of antibiotic drugs and antitumor compounds such as mitomycin C⁸ and anthracyclines.^{9,10} Those quinoid antitumor

drugs are believed to form covalent linkages with DNA bases through QM intermediates.^{9,11} DNA cross-linking, which is probably one of the most important application of QMs reactivity, has been obtained as a result of two consecutive alkylating steps, both involving QMs.¹²

Such a reactivity is mainly due to the QM electrophilic nature, which is remarkable in comparison to that of other neutral electrophiles. In fact, QMs are good Michael acceptors, and nucleophiles add readily under mild conditions at the QM exocyclic methylene group to form benzylic adducts. *o*-QM (**1**) and *p*-QM (**2**) (Scheme 1) are the prototypes of more complex quinone methide-like structures, and they represent simple models which can be used to study the effects of the ortho and para geometries on the reactivity and selectivity.

* Corresponding author. Telephone: +39 0382 507668. Fax: +39 0382 507323. E-mail: freccero@chifis.unipv.it.

(1) *Lignins: Occurrence, Formation, Structure and Reactions*; Sarkanen, K. V., Ludvig, C., Eds.; Wiley: New York, 1971.

(2) Peter, M. G. *Angew. Chem., Int. Ed. Engl.* **1989**, *28*, 555 and references therein.

(3) McDonald, I. A.; Nyce, P. L.; Jung, M. J.; Sabol, J. S. *Tetrahedron Lett.* **1991**, *32*, 887.

(4) Wang, Q.; Dechert, U.; Jirik, F.; Withers, S. G. *Biochem. Biophys. Res. Commun.* **1994**, *200*, 577.

(5) Cabaret, D.; Adediran, S. A.; Garcia Gonzales, M. J.; Pratt, R. F.; Wakselman, M. J. *Org. Chem.* **1999**, *64*, 713.

(6) Myers, J. K.; Cohen, J. D.; Widlanski, T. S. *J. Am. Chem. Soc.* **1995**, *117*, 11049.

(7) Stowell, J. K.; Widlanski, T. S.; Kutateladze, T. G.; Raines, R. T. *J. Org. Chem.* **1995**, *60*, 6930.

(8) (a) Tomasz, M.; Das, A.; Tang, K. S.; Ford, M. G. J.; Minnock, A.; Musser, S.; Waring, M. J. *J. Am. Chem. Soc.* **1998**, *120*, 11581. (b) Han, I.; Russel, J.; Kohn, H. *J. Org. Chem.* **1992**, *57*, 1799.

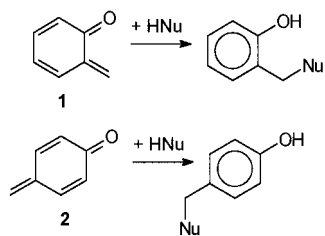
(9) Gaudiano, G.; Frigerio, M.; Bravo, P.; Koch T. H. *J. Am. Chem. Soc.* **1990**, *112*, 6704.

(10) Angle, S. R.; Rainier, J. D.; Woytowicz C. *J. Org. Chem.* **1997**, *62*, 5884.

(11) Ouyang, A.; Skibo, E. B. *J. Org. Chem.* **1998**, *63*, 1893 and references therein.

(12) (a) Zeng, Q.; Rokita, S. E. *J. Org. Chem.* **1996**, *61*, 9080. (b) Nakatani, K.; Higashida, N.; Saito, I. *Tetrahedron Lett.* **1997**, *38*, 5005.

Scheme 1



Alkylations of simple sulfur-, nitrogen-, and oxygen-centered nucleophiles by quinone methides have experimentally been investigated.^{13–15} More recently, their reactivity has been studied with biological nucleophiles such as free amino acids,^{15,16,17a} oligopeptides,^{15–17} and nucleobases.^{18–20}

The understanding of the relationships between QM structural modifications, solvent effects (including both specific interactions, such as H-bonding with the alkylated substrates and bulk effects), and QM reactivity/selectivity is indispensable for designing QM-based drugs that, while active, are however characterized by the lowest possible toxicological and pharmacological side effects.²¹ For instance, it is commonly believed that the shorter the QM half-lives, the lower their hepatotoxic effects.^{16,17b,c}

In general, the selectivity of peptide- or DNA-alkylating agents is the result of their selective preassociation with the biological substrate directed by a specific structure of their chemical precursors. The selectivity of the reaction is less frequently determined by a specific characteristic of the electrophilic moiety of the alkylating agents; however, when this aspect is important, as in the case of QMs, it should be thoroughly investigated. A full understanding of this aspect will allow an improved explanation of their chemical and pharmacological activities.

Experimental data demonstrate that reactivity and selectivity in the reaction of QMs with biological nucleophiles can be highly sensitive to (i) modification of the electrophile structure²² and (ii) the protonation of the carbonyl moiety.^{17,20} In fact, both reactivity and selectivity of QM alkylation reactions can be enhanced by hydrogen bonding involving the QM carbonyl oxygen²⁰ and either a protic solvent such as water²³ or Brønsted

acid^{23a,c,24} and acidic hydrogen atoms in peptides and in DNA nucleobases.^{18–20} Shielding of the carbonyl oxygen from such a solvent interaction has been suggested as the cause of the low reactivity of crowded *p*-QMs (with hydrophobic substituents at the 2- and 6-positions).^{17,20}

Although research on QMs as biological alkylating agents is at present very active on the experimental side, no computational investigation focused on the effect of structural features, H-bonding, and solvent effect on the QM-reactivity/selectivity has appeared to date in the literature. The pioneering investigation by Soucek et al. based on the HMO method is, to our knowledge, the first and only attempt to predict the stability (and thus to some extent the reactivity) of several *p*- and *o*-quinone methides.^{22b}

Concerning related nucleophilic addition to α,β -unsaturated carbonyl compounds, previous ab initio computational studies have been reported for the Michael addition of anionic nucleophiles^{25–27} to “classical activated double bonds” (acrolein, acrylonitrile, maleimide, acrylic and methacrylic acids). Although, in a biological environment, nucleophiles exist mainly in the undissociated form, only two computational studies addressed the 1,4-addition to activated double bonds with neutral nucleophiles such as ammonia²⁸ and dimethylamine.²⁹

QMs are much less stable and much more reactive alkylating agents than classical electron-poor olefin, and a generalization of the results obtained for the alkylation of ammonia by acrolein and acrylic acids to QMs is probably not appropriate.

The highest experimental reactivity of *o*-QM among other QMs and its unexpected high selectivity in the alkylation of amino acids¹⁵ and nucleobases^{18–20} (dC, dA, and dG) prompted us to investigate in more detail the general sensitivity of the electrophile to protonation and the role of its ortho geometry. Thus, we report a thorough computational DFT investigation on the alkylation reaction of prototype nucleophiles (ammonia and hydrogen sulfide) by *o*-QM, in competition with its hydration reaction in water. In particular, we will clarify the role of the protic solvent water and the hydrogen bonding between *o*-QM and the substrate (being alkylated) in the control of its reactivity.

Our study is also aimed at validating an affordable and reliable computational method to deal with the selectivity of QM alkylation with polyfunctional biological nucleophiles. Actually, it is part of a systematic experimental and computational investigation, currently in progress in our laboratory, on the electrophilic alkylation of enzymes and nucleobases with QMs.

Computational Details

All calculations were carried out using the Gaussian 94³⁰ and Gaussian 98³¹ program packages.

(24) (a) Zhou, Q.; Turnbull, K. D. *J. Org. Chem.* **1999**, *64*, 2847. (b) Zhou, Q.; Turnbull, K. D. *J. Org. Chem.* **2000**, *65*, 2022.

(25) Wong, S. S.; Paddon-Row, M. N.; Li, Y.; Houk, K. N. *J. Am. Chem. Soc.* **1990**, *112*, 8679.

(26) Osman, R.; Namboodire, K.; Weinstein, H.; Rabinowitz, J. R. *J. Am. Chem. Soc.* **1988**, *110*, 1701.

(27) Thomas, B. E.; Kollman, P. A. *J. Org. Chem.* **1995**, *60*, 8375.

(28) Pardo, L.; Osman, R.; Weinstein, H.; Rabinowitz, J. R. *J. Am. Chem. Soc.* **1993**, *115*, 8263.

(29) Okumoto, S.; Yamabe, S. *J. Org. Chem.* **2000**, *65*, 1544.

(30) Frisch, M. J.; Trucks, G. W.; Schlegel, H. B.; Gill, P. M. W.; Johnson, B. G.; Robb, M. A.; Cheeseman, J. R.; Keith, T.; Petersson, G. A.; Montgomery, J. A.; Raghavachari, K.; Al-Laham, M. A.; Zakrzewski, V. G.; Ortiz, J. V.; Foresman, J. B.; Cioslowski, J.; Stefanov, B. B.; Nanayakkara, A.; Challacombe, M.; Peng, C. Y.; Ayala, P. Y.; Chen, W.; Wong, M. W.; Andres, J. L.; Replogle, E. S.; Gomperts, R.; Martin, R. L.; Fox, D. J.; Binkley, J. S.; Defrees, D. J.; Baker, J.; Stewart, J. P.; Head-Gordon, M.; Gonzalez, C.; Pople, J. A. *Gaussian 94*, Revision E.3; Gaussian, Inc.: Pittsburgh, PA, 1995.

(13) Leary, G.; Miller, I. J.; Thomas, W.; Woolhouse, A. D. *J. Chem. Soc., Perkin Trans. 2* **1977**, 1737.

(14) Gardner, P. D.; Sarrafzadeh Rafsanjani H.; Rand, L. *J. Am. Chem. Soc.* **1959**, *81*, 3364.

(15) Modica, E.; Zanaletti, R.; Freccero, M.; Mella, M. *J. Org. Chem.* **2001**, *66*, 41–52.

(16) McCracken, P. G.; Bolton, J. L.; Thatcher, G. R. J. *J. Org. Chem.* **1997**, *62*, 1820.

(17) (a) Bolton, J. L.; Turnipseed, S. B.; Thompson, J. A. *Chem.-Biol. Interact.* **1997**, *107*, 185. (b) Bolton, J. L.; Valerio, L. G.; Thompson, J. A. *Chem. Res. Toxicol.* **1992**, *5*, 816. (c) Thompson, D. C.; Perera, K.; Krol, E. S.; Bolton, J. L. *Chem. Res. Toxicol.* **1995**, *8*, 323.

(18) Rokita, S. E.; Yang, J.; Pande, P.; Shearer, J.; Greenberg, W. A. *J. Org. Chem.* **1997**, *62*, 3010.

(19) Pande, P.; Shearer, J.; Yang, J.; Greenberg, W. A.; Rokita, S. E. *J. Am. Chem. Soc.* **1999**, *121*, 6773.

(20) Lewis, M. A.; Graff Yoerg, D.; Bolton, J. L.; Thompson, J. A. *Chem. Res. Toxicol.* **1996**, *9*, 1368.

(21) Thompson, D. C.; Thompson, J. A.; Sugumaran, M.; Moldéus, P. *Chem.-Biol. Interact.* **1992**, *86*, 129.

(22) (a) Velek, J.; Koutek, B.; Musil, L.; Vasickova, S.; Soucek, M. *Collect. Czech. Chem. Commun.* **1981**, *46*, 873. (b) Musil, L.; Koutek, B.; Pisova, M.; Soucek, M. *Collect. Czech. Chem. Commun.* **1981**, *46*, 1148. (c) Koutek, B.; Pisova, M.; Krupicka, J.; Lycka, A.; Snobl, D.; Soucek, M. *Collect. Czech. Chem. Commun.* **1982**, *47*, 1645.

(23) (a) Wan, P.; Barker, B.; Diao, L.; Fisher, M.; Shi, Y.; Yang, C. *Can. J. Chem.* **1996**, *74*, 465. (b) Diao, L.; Cheng, Y.; Wan, P. *J. Am. Chem. Soc.* **1995**, *117*, 5369. (c) Brousmiche, D.; Wan, P. *Chem. Commun.* **1998**, 491.

Reactants, intermediates (**I**), transition structures (**S**), and products (**P**) have been optimized by the B3LYP method, using 6-31G(d) and 6-311+G(d,p) basis sets. To assess the reliability of a basis set in describing the geometries of the stationary points, we optimized an intermediate (**I1**) and three TSs, namely **S1**, **S2in**, and **S3in**, at the B3LYP/AUG-cc-pVTZ level. B3LYP/6-311+G(d,p) optimized geometries were used for systematic single-point calculations at the B3LYP/AUG-cc-pVTZ level. Stationary points for the alkylation reaction involving hydrogen sulfide have also been optimized with B3LYP using the 6-311+G(d,p) basis set extended with a further d-type function and an f-type function on the S atom [hereafter referred to as 6-311+G(d,p),S(2df)]. The extension of the S atom basis set is suggested to achieve a better treatment of stationary points containing S atoms.³²

Intrinsic reaction coordinate (IRC) calculations were performed [at the B3LYP/6-31+G(d,p) level for ammonia and water nucleophiles and at the B3LYP/6-31+G(d,p),S(3df) level for hydrogen sulfide alkylation reaction] in order to connect the TSs to precomplexed reagents and products and to investigate in detail the alkylation process as a function of the nucleophile features.

To confirm the nature of the stationary points and to produce theoretical activation parameters, vibrational frequencies (in the harmonic approximation) were calculated for all the optimized B3LYP/6-311+G(d,p) [B3LYP/6-311+G(d,p),S(2df) for stationary points involving a S atom] structures and used, unscaled, to compute the zero-point energies, their thermal corrections, the vibrational entropies, and their contributions to activation enthalpies, entropies, and Gibbs activation free energies. The computed relative electronic energies for complexes and transition structures and the thermodynamic activation parameters [at the B3LYP/6-311+G(d,p) and B3LYP/6-311+G(d,p),S(2df) levels], obtained from gas-phase vibrational frequencies, are listed in Tables 1 and 2, respectively.

The computed enthalpy, entropy, and Gibbs free energy were converted from the 1 atm standard state into the standard state of molar concentration (ideal mixture at 1 mol L⁻¹ and 1 atm) in order to allow a direct comparison with the experimental result in water solution.³³

We have also performed CHelpG charge calculations in order to analyze atomic charges and dipole moments of the stationary points (Table 3).

The contributions of specific and bulk solvent effects to the activation Gibbs free energy of the reactions under study were investigated in two steps. First, a specific water molecule was explicitly included in the gas-phase computation. The solvent was then considered as a macroscopic and continuum medium. Each stationary point has been optimized in solvent at the B3LYP/6-311+G(d,p) level, using the COSMO version of the polarizable continuum model implemented in the Gaussian package (C-PCM).³⁴ The reaction mechanisms, with and

Table 1. Relative Energies (kcal mol⁻¹)^a of the Stationary Points Governing the Reaction between *o*-QM and Nucleophiles without (**1–3**) and with (**4–6**) an Explicit Water Molecule in Vacuum at the B3LYP Level with Different Basis Sets

| structure | B3LYP / AUG-cc-pVTZ// | | | B3LYP / AUG-cc-pVTZ |
|--------------------------------------|-----------------------|----------------------------|--------------------|---------------------|
| | B3LYP/6-31G(d) | B3LYP/6-311+G(d,p) | B3LYP/6-311+G(d,p) | |
| Uncatalyzed Mechanism (Figure 1) | | | | |
| I1 | -6.05 | -4.23 | -3.51 | — |
| I2 | -9.62 | -7.01 | -6.18 | -6.19 |
| I3 | -3.91 | -3.18 (-3.00) ^b | -2.59 | — |
| S1 | 1.58 | 5.13 | 6.28 | 6.29 |
| S2in | 4.03 | 10.29 | 10.65 | 10.65 |
| S2out | 6.06 | 11.64 | 11.81 | — |
| S3in | 7.19 | 7.97 (8.35) ^b | 8.29 | 8.27 |
| S3out | 7.61 | 8.30 (8.57) ^b | 8.39 | — |
| Water-Catalyzed Mechanism (Figure 2) | | | | |
| I4 | -15.64 | -11.66 | -9.81 | — |
| I5 | -19.69 | -15.54 | -13.22 | — |
| I6 | -14.64 | -11.15 | — | — |
| S4 | -14.99 | -9.22 | -6.66 | — |
| S5in | -13.79 | -3.46 | -1.57 | — |
| S5out | -9.86 | -0.26 | 1.28 | — |
| S6in | -4.52 | -0.11 (0.34) ^b | 1.78 | — |
| S6out | -3.39 | 0.88 (1.12) ^b | 2.34 | — |
| Reaction Products (Figure 1) | | | | |
| P1 | -31.90 | -28.77 | — | — |
| P2 | -29.61 | -23.61 | — | — |
| P3 | -28.73 | -28.89 | — | — |

^a Relative to the isolated reactants, whose energies (Hartree) are -76.4089533 (H₂O), -56.5479473 (NH₃), -399.3854386 (H₂S), -345.5358169 (**1**) (B3LYP/6-31G(d)); -76.4584638 (H₂O), -56.582636 (NH₃), -399.4225308 (H₂S), -345.6315701 (**1**) (B3LYP/6-311+G(d,p)); -76.4661979 (H₂O), -56.5888217 (NH₃), -399.432261 (H₂S), -345.6651090 (**1**) [single-point calculations, B3LYP/AUG-cc-pVTZ//B3LYP/6-311+G(d,p)]; -76.466198 (H₂O), -56.5888577 (NH₃), -399.4322644 (H₂S), -345.6652194 (**1**) (B3LYP/AUG-cc-pVTZ).
^b Stationary points containing a S atom optimized at the B3LYP/6-311+G(d,p),S(2df) level.

without an explicit water molecule, have been investigated in order to clarify the role of both protonation and bulk effects of water on the *o*-QM reactivity as alkylating agent.

Results and Discussion

The Choice of the Basis Set. The most relevant geometrical parameters of all stationary points, without and with addition of an explicit water molecule, located at B3LYP/6-31G(d) and B3LYP/6-311+G(d,p) [B3LYP/6-311+G(d,p),S(2df) for stationary points with a sulfur atom] levels on the potential energy surface describing the alkylation of ammonia, water, and hydrogen sulfide by *o*-QM (**1**) are gathered in Figures 1 and 2.

The corresponding relative (to free reactants) energies are listed in Table 1, and some additional information concerning electronic features (charges, charge transfers, and dipole moments) is given in Table 3.

From a geometrical point of view, the enlargement of the basis set from 6-31G(d) to 6-311+G(d,p) does not change TS-forming bond lengths by more than 0.13 Å, while pre-reaction cluster geometries (**I1–I6**) are more affected by basis set choice. Moreover, on passing from 6-31G(d) to 6-311+G(d,p), both intermediate and TS geometries become more reliable, at least as judged from a comparison with the corresponding AUG-cc-pVTZ geometries. In fact, we demonstrated that geometrical features of stationary points (such as **I2** and **S1–S3**) optimized

(31) Frisch, M. J.; Trucks, G. W.; Schlegel, H. B.; Scuseria, G. E.; Robb, M. A.; Cheeseman, J. R.; Zakrzewski, V. G.; Montgomery, J. A., Jr.; Stratmann, R. E.; Burant, J. C.; Dapprich, S.; Millam, J. M.; Daniels, A. D.; Kudin, K. N.; Strain, M. C.; Farkas, O.; Tomasi, J.; Barone, V.; Cossi, M.; Cammi, R.; Mennucci, B.; Pomelli, C.; Adamo, C.; Clifford, S.; Ochterski, J.; Petersson, G. A.; Ayala, P. Y.; Cui, Q.; Morokuma, K.; Malick, D. K.; Rabuck, A. D.; Raghavachari, K.; Foresman, J. B.; Cioslowski, J.; Ortiz, J. V.; Stefanov, B. B.; Liu, G.; Liashenko, A.; Piskorz, P.; Komaromi, I.; Gomperts, R.; Martin, R. L.; Fox, D. J.; Keith, T.; Al-Laham, M. A.; Peng, C. Y.; Nanayakkara, A.; Gonzalez, C.; Challacombe, M.; Gill, P. M. W.; Johnson, B. G.; Chen, W.; Wong, M. W.; Andres, J. L.; Head-Gordon, M.; Replogle, E. S.; Pople, J. A. *Gaussian 98*, Revision A.7; Gaussian, Inc.: Pittsburgh, PA, 1998.

(32) (a) Arnaud, R.; Juvin, P.; Vallée, Y. *J. Org. Chem.* **1999**, *64*, 8880. (b) Rutting, P. J.; Burgers, P. C.; Francis, J. T.; Terlouw, J. K. *J. Phys. Chem.* **1996**, *100*, 9694.

(33) For conversion from 1 atm standard state to 1 mol/L standard state, the following contributions need to be added to standard enthalpy, entropy, and Gibbs free energy: $-RT$, $-R - R \ln R/T$, and $RT \ln R/T$, where R is the value of R in L × atm/mol × K (ref 45). For a reaction with A + B = C stoichiometry (such as the unassisted alkylation mechanism, Figure 1), the corrections for ΔH^\ddagger , ΔS^\ddagger , and ΔG^\ddagger are RT , $R + R \ln R/T$, and $RT \ln R/T$. At 298 K, the corrections amount to 0.59 and -1.90 kcal mol⁻¹ for ΔH^\ddagger and ΔG^\ddagger and +8.34 eu for ΔS^\ddagger (ref 46). For a reaction with A + B + C = D stoichiometry (such as the water-assisted alkylation mechanism, Figure 2), the corrections for ΔH^\ddagger , ΔS^\ddagger , and ΔG^\ddagger are $2RT$, $2(R + R \ln R/T)$, and $2RT \ln R/T$. At 298 K, the corrections amount to 1.18 and -3.79 kcal mol⁻¹ for ΔH^\ddagger and ΔG^\ddagger and +16.68 eu for ΔS^\ddagger .

(34) (a) Cramer, C. J.; Truhlar, D. G. *Chem Rev.* **1999**, *99*, 2161. (b) Barone, V.; Cossi, M. *J. Phys. Chem.* **1998**, *102*, 1995.

Table 2. B3LYP/6-311+G(d,p) Thermodynamic Parameters (ΔH , $-\Delta S$, ΔG_{gas}),^a Solvent Effect on the Stationary Points (δG , kcal mol⁻¹),^b and Solvent Effect on the Alkylation Reactions ($\Delta\Delta G$, kcal mol⁻¹)^c of NH₃, H₂O, and H₂S by *o*-QM, without and with an Explicit Water Molecule at 298.15 K

| structure | ΔH | $-\Delta S$ | ΔG_{gas} | δG^b | $\delta\Delta G^c$ | ΔG_{sol}^d |
|--------------------------------------|----------------------|----------------------|-------------------------|-----------------------|----------------------|---------------------------|
| Uncatalyzed Mechanism (Figure 1) | | | | | | |
| I1 | -2.14 | 5.14 | 3.00 | -3.48 | 4.96 | 7.96 |
| | — | — | — | (-3.59) ^e | (5.05) ^e | (8.05) ^e |
| I2 | -4.79 | 5.57 | 0.78 | -4.83 | 5.86 | 6.64 |
| | — | — | — | (-5.07) ^e | (5.84) ^e | (6.62) ^e |
| I3 | -1.24 | 4.04 | 2.80 | -0.10 | 4.26 | 7.06 |
| | (-1.07) ^f | (4.00) ^f | (2.93) ^f | — | — | — |
| | | | | (-0.64) ^e | (3.88) ^e | (6.68) ^e |
| S1 | 7.17 | 8.61 | 15.78 | -12.04 | -3.60 | 12.18 |
| | — | — | — | (-12.55) ^e | (-3.91) ^e | (11.87) ^e |
| S2in | 11.39 | 9.40 | 20.79 | -8.46 | 2.23 | 23.02 |
| | — | — | — | (-9.05) ^e | (1.86) ^e | (22.65) ^e |
| S2out | 12.52 | 9.42 | 21.94 | -9.32 | 1.37 | 23.31 |
| | — | — | — | (-10.04) ^e | (0.87) ^e | (22.81) ^e |
| S3in | 8.15 | 9.03 | 17.18 | -2.33 | 2.02 | 19.20 |
| | (8.58) ^f | (9.01) ^f | (17.59) ^f | — | — | (19.61) ^f |
| | — | — | — | (-2.59) ^e | (1.93) ^e | (19.11) ^e |
| S3out | 8.43 | 8.98 | 17.41 | -2.56 | 1.80 | 19.21 |
| | (8.62) ^f | (8.98) ^f | (17.61) ^f | — | — | (19.41) ^f |
| | — | — | — | (-2.86) ^e | (1.66) ^e | (19.07) ^e |
| Water-Catalyzed Mechanism (Figure 2) | | | | | | |
| I4 | -7.30 | 11.22 | 3.92 | -4.33 | 10.81 | 14.72 |
| I5 | -10.89 | 11.68 | 0.78 | -5.31 | 12.08 | 12.86 |
| I6 | -6.94 | 9.81 | 2.87 | -1.33 | 9.73 | 12.60 |
| S4 | -4.92 | 15.13 | 10.21 | -10.14 | 5.00 | 15.21 |
| | — | — | — | (-6.75) ^e | (8.66) ^e | (18.87) ^e |
| S5in | -0.10 | 16.92 | 16.82 | -11.94 | 5.45 | 22.27 |
| | — | — | — | (-12.03) ^e | (5.65) ^e | (22.47) ^e |
| S5out | 2.35 | 17.00 | 19.35 | -14.56 | 2.83 | 22.18 |
| | — | — | — | (-14.74) ^e | (2.94) ^e | (22.29) ^e |
| S6in | 1.57 | 16.41 | 17.98 | -4.87 | 6.19 | 24.17 |
| | (2.18) ^f | (16.42) ^f | (18.60) ^f | — | — | (24.79) ^f |
| | — | — | — | (-5.84) ^e | (5.45) ^e | (23.43) ^e |
| S6out | 2.33 | 16.26 | 18.59 | -5.52 | 5.54 | 24.13 |
| | (2.68) ^f | (16.26) ^f | (18.94) ^f | — | — | (24.48) ^f |
| | — | — | — | (-6.83) ^e | (4.46) ^e | (23.05) ^e |
| Reaction Products (Figure 1) | | | | | | |
| P1 | -24.51 | 9.28 | -15.23 | — | — | — |
| P2 | -19.37 | 8.88 | -10.49 | — | — | — |
| P3 | -23.91 | 8.94 | -14.97 | — | — | — |

^a With respect to reactants, whose kinetic contributions (non-potential-energy terms) to molar entropy ($T\Delta S$), enthalpy (δH), and Gibbs free energy (δG) are 13.44 (H₂O), 13.71 (NH₃), 14.66 (H₂S), 14.65 (H₂S, at B3LYP/6-311+G(d,p)S(2df)), 50.36 (**I**); 15.73 (H₂O), 23.88(NH₃), 11.79 (H₂S), 11.78 (H₂S, at B3LYP/6-311+G(d,p)S(2df)), 72.662 (**I**); 2.29 (H₂O), 10.17 (NH₃), -2.87 (H₂S), -2.87 (H₂S, at B3LYP/6-311+G(d,p)S(2df)), 48.73 (**I**), respectively (kcal mol⁻¹). Symmetry numbers used to calculate entropy are $\sigma = 1$ for **I**, $\sigma = 2$ for H₂O, H₂S and $\sigma = 3$ for NH₃. A correction of $R \ln 2$ to ΔS has been added for the alkylation reactions, as the nucleophile attacks to *o*-QM faces are not experimentally distinguishable. ^b Solvent effect on intermediates and TSs by C-PCM single-point calculations on gas-phase geometries B3LYP-C-PCM/6-311+G(d,p)//B3LYP/6-311+G(d,p). Solvent effects on reactants (δG_{react}) by C-PCM single-point calculations on gas-phase geometries are -6.70 (H₂O), -4.45 (NH₃), -0.37 (H₂S), -3.99 (**I**). Solvent effects on optimized reactants in water (δG_{react}) are -6.77 (H₂O), -4.50 (NH₃), -0.38 (H₂S), -4.14 (**I**). ^c Solvent effect on reaction Gibbs free energy, calculated as $\delta\Delta G = \delta G - \delta G_{\text{react}}$. ^d Gibbs free energy in water solution calculated as $\Delta G_{\text{sol}} = \Delta G_{\text{gas}} + \delta\Delta G$. ^e Solvent effect on optimized stationary points in water calculated at the B3LYP-C-PCM/6-311+G(d,p) level. ^f Optimization and frequency calculations for stationary points containing a S atom performed at the B3LYP/6-311+G(d,p),S(2df) level.

at 6-311+G(d,p) are very similar to those obtained with the very good (but too time-consuming) AUG-cc-pVTZ basis.³⁵

Energies, as expected, are much more basis set dependent than geometries. Thus, activation energies of TSs and formation

Table 3. Charge (CHelpG) on *o*-QM Oxygen Atom, Charge Transfer (q) from Nucleophile to *o*-QM (in Electrons), Dipole Moment (μ , in Debye) in a Vacuum and in Water Solution for the Alkylation Reactions at the B3LYP/6-311+G(d,p) Level

| structure | charge on <i>o</i> -QM | | | |
|--------------------------------------|------------------------|--------------|-----------------------------|------------------------------|
| | oxygen atom (CHelpG) | q (CHelpG) | μ (vacuum) ^a | μ (water) ^{b,c} |
| <i>o</i> -QM | -0.56 | — | 3.60 | 5.11 (5.28) ^d |
| Uncatalyzed Mechanism (Figure 1) | | | | |
| I1 | -0.59 | 0.00 | 2.48 | 3.54 (3.88) ^d |
| I2 | -0.59 | -0.04 | 3.73 | 4.91 (5.41) ^d |
| I3 | -0.59 | 0.00 | 4.83 | 6.11 (6.49) ^d |
| S1 | -0.65 | -0.30 | 5.01 | 7.41 (7.57) ^d |
| S2in | -0.67 | -0.17 | 3.46 | 4.95 (5.44) ^d |
| S2out | -0.71 | -0.18 | 3.32 | 4.84 (5.25) ^d |
| S3in | -0.63 | -0.13 | 3.21 | 4.51 (4.65) ^d |
| S3out | -0.68 | -0.13 | 3.32 | 4.84 (4.12) ^d |
| Water-Catalyzed Mechanism (Figure 2) | | | | |
| I4 | -0.64 | -0.04 | 2.38 | 3.41 |
| I5 | -0.63 | +0.05 | 3.44 | 4.46 |
| I6 | -0.60 | 0.00 | 4.77 | 5.85 |
| S4 | -0.69 | -0.28 | 4.37 | 6.62 (3.86) ^d |
| S5in | -0.77 | -0.25 | 3.45 | 5.43 (5.25) ^d |
| S5out | -0.56 | -0.25 | 5.09 | 7.48 (7.40) ^d |
| S6in | -0.79 | -0.19 | 1.68 | 2.81 (5.33) ^d |
| S6out | -0.81 | -0.19 | 2.58 | 3.84 (6.67) ^d |

^a Nucleophile dipole moments (in debye) in the gas phase are as follows: 2.16 (H₂O), 1.70 (NH₃), 1.35 (H₂S). ^b Nucleophile dipole moments in water by single-point calculation are as follows: 2.49 (H₂O), 2.06 (NH₃), 1.61 (H₂S). Nucleophile dipole moments optimized in water are as follows: 2.51 (H₂O), 2.16 (NH₃), 1.61 (H₂S). ^c Calculated by single-point method on gas-phase geometries at the B3LYP-C-PCM/6-311+G(d,p)//B3LYP/6-311+G(d,p) level. ^d Calculated by optimization of the stationary points in water at the B3LYP-C-PCM/6-311+G(d,p) level.

energies of intermediates change considerably on passing from 6-31G(d) to 6-311+G(d,p) basis sets. However, a further enlargement of the basis set, namely on passing from 6-311+G(d,p) to AUG-cc-pVTZ basis, is accompanied by a much smaller variation in activation energies (less than 2.5 kcal mol⁻¹), and, even more important, the difference between activation energies of TSs (i.e., **S1**, **S2**, and **S3in**) does not change appreciably (see Table 1). Moreover, it is remarkable that B3LYP/AUG-cc-pVTZ//B3LYP/6-311+G(d,p) single-point activation energies for these TSs differ from fully optimized B3LYP/AUG-cc-pVTZ activation energies by less than 0.03 kcal mol⁻¹.

This observation suggests that refining energies by single-point calculations with the AUG-cc-pVTZ basis set on 6-311+G(d,p) optimized geometries is a reliable practice, and this method was adopted by us for all stationary points reported in this paper. In the discussion we will refer, unless otherwise stated, to B3LYP/6-311+G(d,p) optimized geometries and to single-point potential energies [B3LYP/AUG-cc-pVTZ//B3LYP/6-311+G(d,p)].

Reactivity in the Gas Phase. “Nucleophilic” vs “Electrophilic” Addition to *o*-QM. (a) Ammonia Alkylation. Let us now summarize the results for the alkylation reaction of ammonia by *o*-QM. The first stationary point located on the potential energy surface is a minimum (more stable than reactants by -3.5 kcal mol⁻¹) corresponding to complex **I1** (Figure 1), where NH₃ is involved in weak H-bonding (hydrogen bond length H - -O of 2.17 Å and N-H - -O angle 156°) to *o*-QM. But, such an intermediate (**I1**) is unstable (+3.0 kcal

(35) AUG-cc-pVTZ basis sets have recently been suggested (in the epoxidation of allylic alcohols by peroxy acids) to be proper for hydrogen-bonding description (Adam, W.; Bach, R. D.; Dmitrenko, O.; Saha-Moller, C. R. *J. Org. Chem.* **2000**, *65*, 6715). However, they are highly time-consuming in the optimization of stationary points.

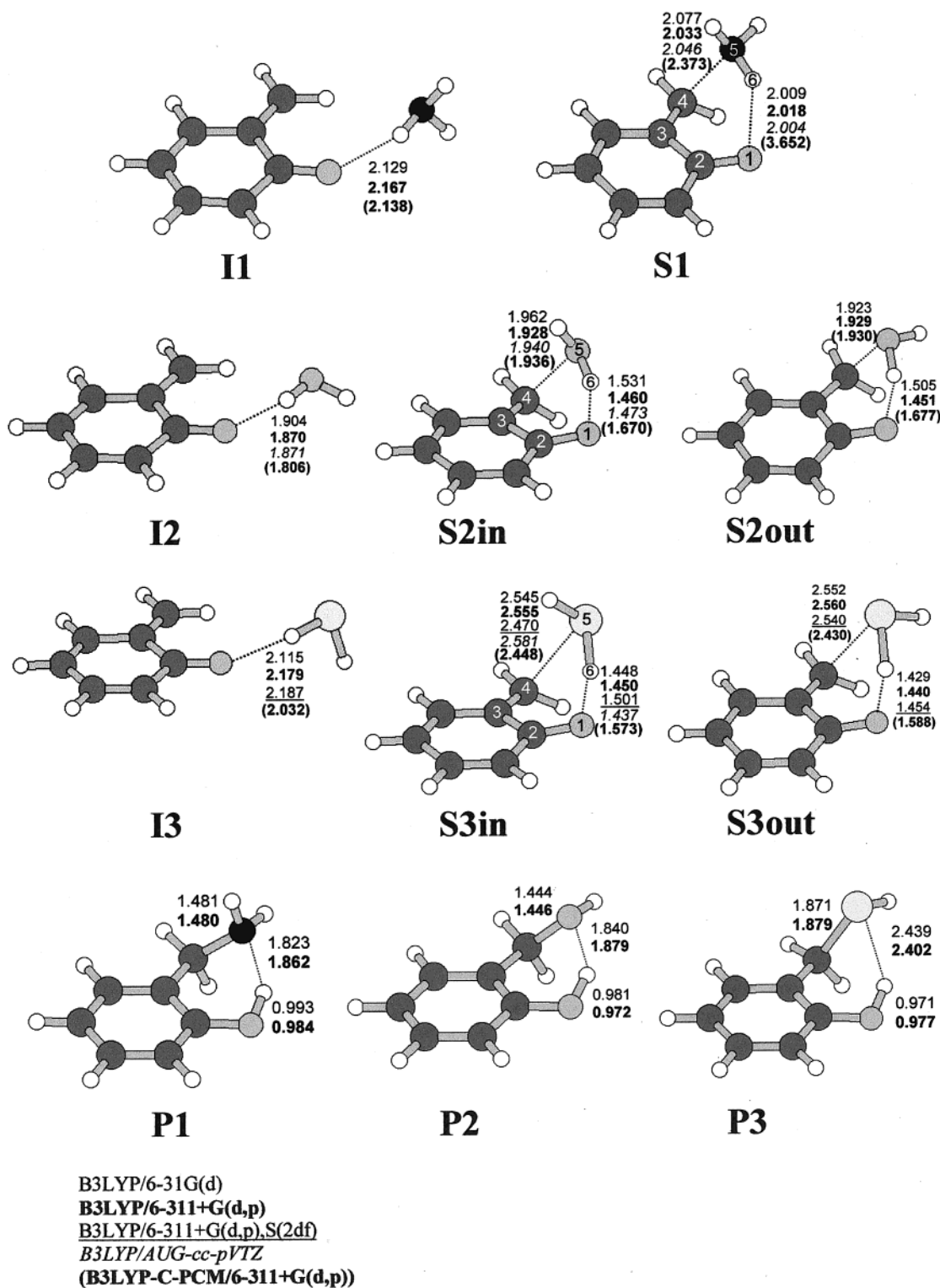


Figure 1. Optimized geometries of prereaction clusters (reactant-like complexes) (**I1**–**I3**), TSs (**S1**–**S3**), and products (**P1**–**P3**) of the NH_3 , H_2O , and H_2S addition to *o*-QM without water catalysis. Bond lengths (in Å) at the B3LYP/6-31G(d) (plain characters), B3LYP/6-311+G(d,p) (bold), B3LYP/6-311+G(d,p),S(2df) (plain underlined characters), B3LYP/AUG-cc-pVTZ (italic), and B3LYP-C-PCM/6-311+G(d,p) (bold characters, in parentheses) levels are reported.

mol^{-1} , see Table 2) when Gibbs free energies are considered. **I1** evolves to the product [2-aminomethyl-phenol (**P1**), which is $-28.8 \text{ kcal mol}^{-1}$ more stable than reactants] through the **S1** TS with a $6.3 \text{ kcal mol}^{-1}$ energy barrier.³⁶

S1 shows $\text{N}_5\text{--H}_6\text{--O}_1$ hydrogen-bonding with a $\text{H}_6\text{--O}_1$ distance of 2.02 \AA , a $\text{N}_5\text{--H}_6\text{--O}_1$ angle of 140.3° , and the forming $\text{C}_4\text{--N}_5$ bond length of 2.03 \AA (see Figure 1 for numbering). Full characterization of **S1** by frequency and IRC

calculations allowed us to identify several features of the ammonia alkylation TS by *o*-QM. First, in **S1** the reaction coordinate vector is almost localized at the $\text{C}_4\text{--N}_5$ bond formation and no proton (H_6) transfer process, from the nitrogen (N_5) to the oxygen atom (O_1), is involved. Second, IRC calculation [at the B3LYP/6-31+G(d,p) level, see Figure 3a] confirms that the proton transfer from ammonia to the QM oxygen occurs much later than the $\text{C}_4\text{--N}_5$ bond formation. In

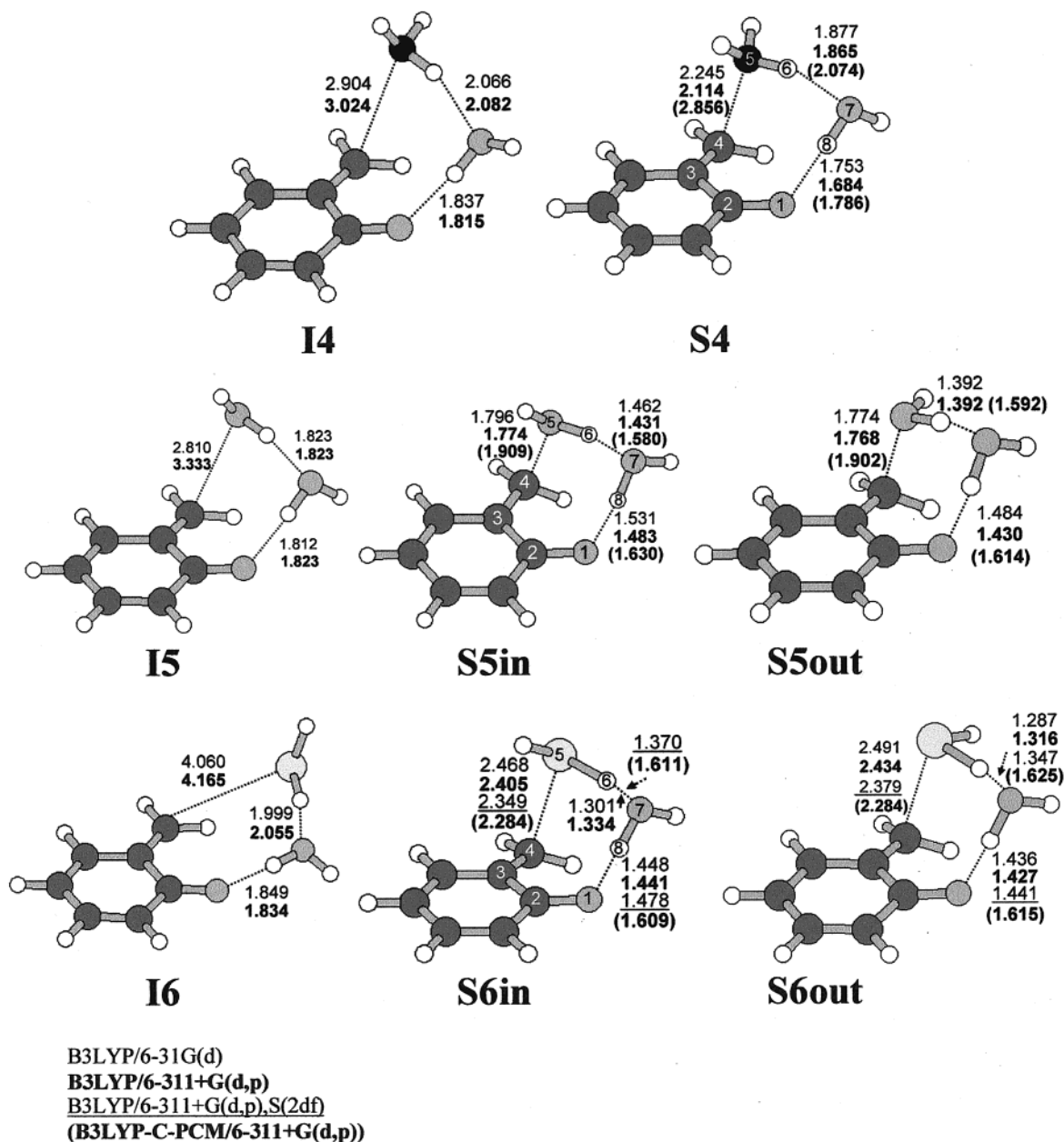


Figure 2. Optimized prereaction clusters (reactant-like complexes) (**I4–I6**), and TSs (**S4–S6**) of the NH_3 , H_2O , and H_2S addition to *o*-QM, including an explicit water molecule (water-assisted mechanism). Bond lengths (in Å) at the B3LYP/6-31G(d) (plain characters), B3LYP/6-311+G(d,p) (bold), B3LYP/6-311+G(d,p),S(2df) (plain underlined characters), and B3LYP-C-PCM/6-311+G(d,p) (bold characters, in parentheses) levels are reported.

fact, at the last point of the IRC (see Figure 3a), the $\text{C}_4\text{--N}_5$ bond is almost completely formed, while the $\text{H}_6\text{--O}_1$ bond is still very long and the $\text{N}_5\text{--H}_6$ is far from being broken.

The structure of TS **S1** is consistent with the accepted “pure nucleophilic addition” to activated double bonds and is quite similar to cyclic TSs identified by Weinstein in a similar study on the 1,4-addition of ammonia on acrolein and acrylic acid (*s-cis* isomers), where the ammonia adds to the β carbon atom without significant proton transfer to the carbonyl oxygen.²⁸

(36) The reactivity of *o*-QM as electrophile is higher than that of “classical” activated double bonds, such as acrylonitrile,²⁸ since *o*-QM alkylation reactions benefits from aromatic ring formation. The analysis of the geometric change of the six-membered ring allows an evaluation of the aromaticity gained at the TSs. The change of a ring bond length, for instance $\text{C}_2\text{--C}_3$ (see Figure 1 for numbering) passing from *o*-QM (1.514 Å) to **S1** TS (1.466 Å) in comparison to the shortening of the same bond from the reactant to the product **P1** (1.413 Å) suggests that approximately 50% of the whole aromaticity has been gained by the reactant at the TSs.

The absence of the “proton-relay component”²⁹ accounts for the zwitterionic character of **S1**. In fact, there is a negative charge increase (−0.1 e) at the QM oxygen atom as a result of NH_3 attack, which parallels the sizable electron transfer from ammonia to *o*-QM (−0.3 e, see Table 3).

The high value of the **S1** dipole moment (5.01 D, in gas phase) and the high negative charge on oxygen atom (−0.65 e) suggest that both polar and protic solvent effects should play a crucial role in the alkylation reaction of nitrogen nucleophiles with *o*-QM. Such a solvent effect should be taken into account for a realistic depiction of the reaction mechanism, particularly in a solvent such as water, which has been used pure or as cosolvent (water/acetonitrile or water/DMF) in numerous experimental investigations focused on QMs as alkylating agents.^{15,17–19}

(b) Water Alkylation. In the exploration of the potential energy surface for the *o*-QM hydration reaction, we located a

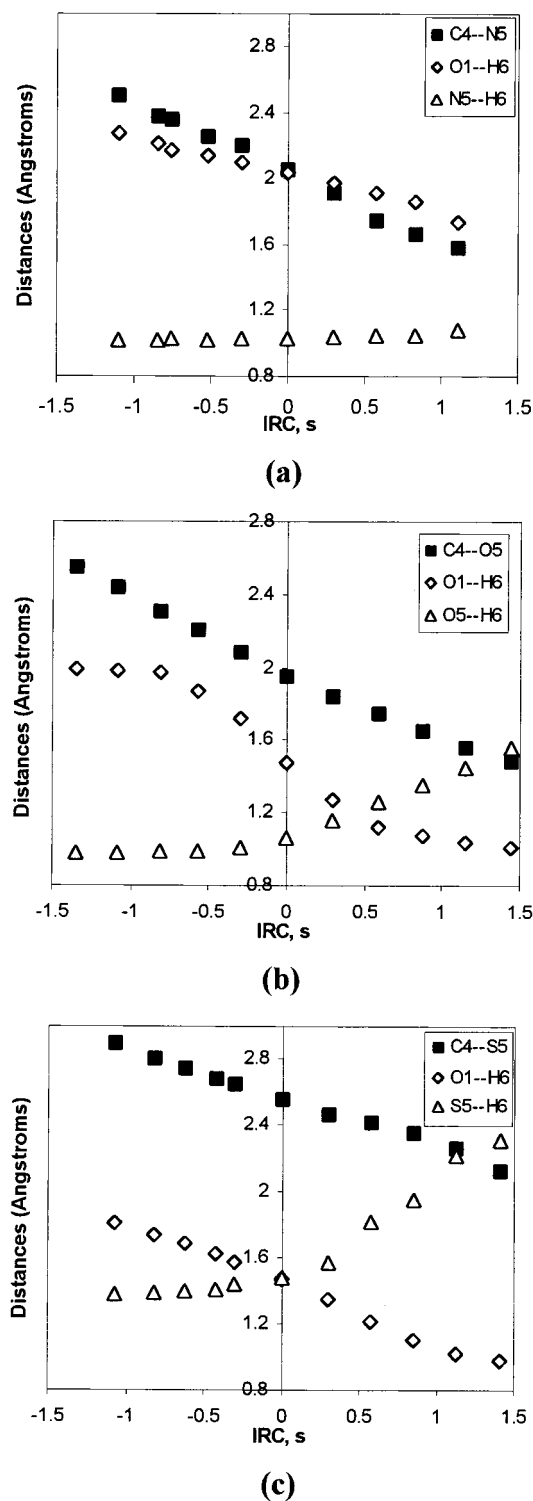


Figure 3. Change of the forming C--nucleophile bond length (■), breaking nucleophile--H bond length (△), and forming O₁--H bond length (◇) along the IRC path starting from **II** [(a) alkylation of NH₃ by *o*-QM, **S1**], **I2** [(b) hydration reaction of *o*-QM, **S2in**] and **I3** [(c) alkylation of H₂S by *o*-QM, **S3in**] to final products **P1**, **P2**, and **P3**, respectively. The IRC calculations have been performed at the B3LYP/6-31+G(d,p) (for N and O nucleophiles) and B3LYP/6-31+G(d,p),S-(3df) (for hydrogen sulfide) levels in the gas phase. The IRC length is given by *s* (amu^{1/2} Bohr), where *s* = 0 represents the transition structures (**S1**, **S2in**, and **S3in**), *s* → ∞ the products.

complex (**I2**) between *o*-QM and water, where H₂O is more strongly bonded to *o*-QM than ammonia. Our results in the gas phase suggest that *o*-QM can give rise to a H-bonded complex

I2 (with a hydrogen bond length of 1.87 Å and a H--O--H angle of 164.1°), which is more stable than free reactants by −6.2 kcal mol^{−1} (Table 1). Inclusion of nonpotential energy terms at 298.15 K allows a proper evaluation of the complexation equilibrium, and it leads to a free energy for complex **I2** only 0.78 kcal mol^{−1} higher [at B3LYP/6-311+G(d,p)] than that for free reactants (see Δ*G*_{gas} in Table 2). Thus, even including an entropic contribution which destabilizes the complex **I2**, calculations suggest that the **I2** concentration, in the gas phase, should be significant.

Other prereaction clusters between reactive alkylating agents and water (such as **I2**) have recently been suggested on the basis of calculations. In fact, in the hydration of formylketene^{37a} and 2,4-cyclohexadien-1-one-6-carbonyl,^{37b} H-bonded complexes have also been located at the MP2/6-31G(d) level, with a potential energy of −5.9 and −6.8 kcal mol^{−1}, respectively, lower than those of the free reactants (entropic terms have been completely neglected in these energy gaps).³⁷

I2 evolves to the product [2-hydroxymethyl-phenol (**P2** in Figure 1), which is −23.6 kcal mol^{−1} more stable than reactants] through a couple of transition states, **S2in** and **S2out**, with activation barriers of 10.7 and 11.8 kcal mol^{−1}, respectively. These TSs differ from each other in the orientation of the water H atom not involved in the H-bonding, which points toward the aromatic ring (inside) in **S2in** and is directed away from it (outside) in **S2out** (Figure 1).

Hydration TSs are tighter than the corresponding ammonia alkylation TS. In fact, **S2in** and **S2out** present a forming bond length of 1.93 Å, slightly shorter than the corresponding one in the alkylation of ammonia (**S1**), and a much stronger O₅--H₆--O₁ hydrogen-bonding (see Figure 1 for numbering), as supported by a H₆--O₁ distance of ~1.46 Å (vs 2.03 Å) and a O₅--H₆--O₁ angle of ~160° (vs N₅--H₆--O₁ 140°).

Full characterization of the most stable **S2in** by frequency and IRC calculations allows us to define such an alkylation as an example of “nucleophilic addition onto *o*-QM assisted by H-bonding” on the basis of the following evidence. **S2in** has only one negative eigenvalue, with the corresponding eigenvector involving formation of both the new C₄--O₅ and O₁--H₆ bonds and breaking of the O₅--H₆ bond. IRC calculation [at B3LYP/6-31+G(d,p) level] shows that, in the *o*-QM hydration reaction, the proton transfer from the water molecule to the *o*-QM oxygen atom occurs much earlier than in the alkylation of NH₃ (see IRC in Figure 3b), and it is almost simultaneous with the formation of the new C₄--O₅ bond. At the TS, lengthening of the O₅--H₆ bond in the water molecule has already started, and shortening of the O₁--H₆ forming bond (involving the carbonyl oxygen of *o*-QM) is “faster” than in the alkylation of ammonia, as clearly reflected in the much steeper slope of the IRC curve (Figure 3b). As a result of the fact that proton transfer takes place in concert with C₄--O₅ bond formation, there is a smaller charge transfer from water to *o*-QM than in **S1** (−0.17 vs −0.30 e), with both TSs **S2in** and **S2out** having a lower dipolar moment (3.46 and 3.32 D, respectively) than **S1**. Thus, apparently, the electrostatic effect of the solvent should play a less important role in the *o*-QM hydration in comparison to the alkylation reaction of nitrogen nucleophiles by *o*-QM.

(c) Hydrogen Sulfide Alkylation. The potential energy surface describing the energetics of hydrogen sulfide alkylation by *o*-QM is qualitatively similar to that of the hydration reaction.

(37) (a) Birney, D. M.; Wagenseller, P. E. *J. Am. Chem. Soc.* **1994**, *116*, 6262. (b) Liu, R., C.-Y.; Luszyk, J.; McAllister, M. A.; Tidwell, T. T.; Wagner, B. D. *J. Am. Chem. Soc.* **1998**, *120*, 6247.

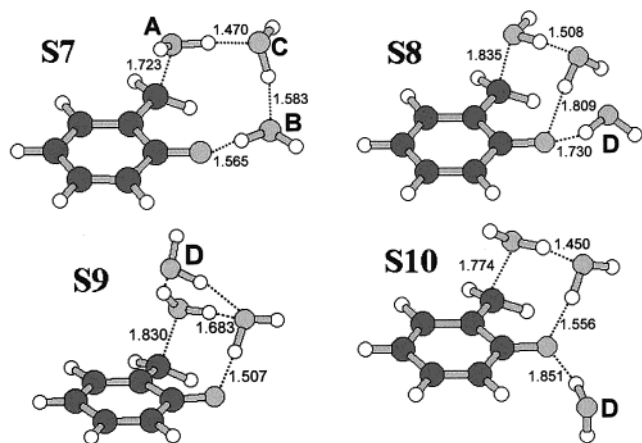
However, important differences exist. We located a prereaction complex (**I3**) between *o*-QM and H₂S only -2.6 kcal mol⁻¹ more stable than the reactants, where hydrogen sulfide is weakly bonded to the carbonyl oxygen. Including non-potential-energy terms, such a complex becomes less stable than free reactants by 2.8 kcal mol⁻¹ (see Table 2). **I3** evolves to the product [2-mercaptomethylphenol, (**P3**) which lies -28.9 kcal mol⁻¹ below the reactants] through two TSs (**S3in** and **S3out**) with very similar activation energies (8.3 and 8.4 kcal mol⁻¹, respectively). Among all of the TSs studied (i.e., **S1**–**S3**), **S3in** and **S3out** show S₅–H₆–O₁ hydrogen-bonding with the shortest H₆–O₁ distance (~ 1.44 Å, with a S₅–H₆–O₁ angle of 165°), and the longest forming C₄–S₅ bond 2.56 Å (see Figure 1 for numbering).

The most striking and interesting difference between **S3** and the TSs located for ammonia alkylation (**S1**) and the hydration reaction (**S2**) is that, in both **S3in** and **S3out**, the major contribution to the reaction coordinate vector arises from the S₅–H₆ internal coordinate (with breaking of the S₅–H₆ bond and formation of the new O₁–H₆ bond with the QM carbonyl oxygen). There is a minor contribution from the C₄–S₅ internal coordinate. IRC calculation [Figure 3c, with the B3LYP/6-31+G(d,p),S(3df) method] confirms that the proton transfer from

(38) Arnaud, R.; Adamo, C.; Cossi, M.; Millet, A.; Vallée, Y.; Barone, V. *J. Am. Chem. Soc.* **2000**, *122*, 324 and references therein.

(39) (a) Yamabe, S.; Ishikawa, T. *J. Org. Chem.* **1997**, *62*, 7049. (b) Yamabe, S.; Ishikawa, T. *J. Org. Chem.* **1999**, *64*, 4519. (c) Okumoto, S.; Fujita N.; Yamabe, S. *J. Phys. Chem.* **1998**, *102*, 3991.

(40) Participation of more than one water molecule in the alkylation reactions of ammonia and water has been suggested by a reviewer as a better prototype of the water-assisted mechanism. In such a supramolecular model, the nucleophile (NH₃ or H₂O, molecule A in TS **S7**) is connected by a H-bonding network to the *o*-QM oxygen atom, through two water molecules. The first one (B) acts as a proton donor and the second one (C), called assistant or “ancillary”, links the nucleophile proton to the other water molecule (see **S7** TS below). This TS geometry should help the reactive system to achieve a better linearity of the hydrogen-bonding network, and therefore should add an additional stabilization. Due to the size and conformational flexibility of such a supramolecular system, calculation at the same level as performed on the prototype reaction model, which involves only one added water molecule, is too time-consuming. Therefore, we decided to investigate this mechanistic hypothesis at the B3LYP/6-31G(d) level for the hydration reaction and for ammonia alkylation in the gas phase. We were able to locate four TSs (**S7**–**S10**) for the water-assisted hydration reaction involving three water molecules.



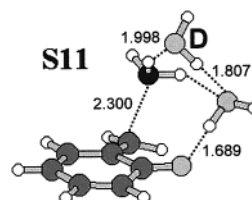
S8–**S10** TSs show geometric features that allows us to qualitatively describe them as **S5**-like TSs with an additional outer water molecule (D). **S8** is the most stable TS, having the lowest electronic energy. **S9** is less stable than **S8** by only 0.56 kcal mol⁻¹. **S7** TS lies 1.48 kcal mol⁻¹ above **S8**, and **S10** is the least stable TS, being 3.1 kcal mol⁻¹ above **S8**. Although **S7** TS displays a geometric array quite similar to that located by Yamabe for the hydrolysis of maleic anhydride,^{39a} a closer inspection reveals the absence of the zwitterionic feature (with the assistant water molecule, C, having a hydronium ion character), which is the peculiar aspect of Yamabe TSs.³⁹ IRC calculations from **S8** (**S9**) and the reaction coordinate vector of **S8**

the H₂S molecule to the *o*-QM oxygen atom (O₁) in **S3in** occurs slightly earlier than in the *o*-QM hydration process, and it appears to be earlier than the C–S bond formation. Shortening of the forming O₁–H₆ bond begins much earlier along the reaction coordinate than in the hydration reaction, as shown by a wider “S-shaped” IRC curve (Figure 3c). Therefore, the above evidence suggests that the alkylation of thiols by *o*-QM proceeds through TSs in which the thiol hydrogen atom exhibits a strong “electrophilic” interaction with the *o*-QM carbonyl oxygen. The lowest nucleophilic character of thiol attack in **S3** TSs as compared to those of ammonia and water in **S1** and **S2** is supported also by the smallest charge transfer (-0.13 e, see Table 3) in the former with respect to the latter.

The Role of Solvation by a Protic Solvent: Reaction of Water-Complexed *o*-QM. It has recently been well documented, mainly by Barone et al., that contemporary continuum models can adequately describe reactions in solution.³⁸ Nevertheless, such an approach would not properly describe the solvent effect on the reactivity if one or more solvent molecules are directly involved in the reaction mechanism.^{28,38,39}

Thus, an appropriate depiction of QM reactivity in water cannot neglect, in principle, both a specific and a bulk effect of

(**S9**) confirm that the proton-transfer process from the nucleophile to the water molecule acting as proton donor does not involve the third water molecule (D). The *o*-QM + *n*H₂O reactions constitute an example of a Curtin–Hammett system.⁴⁷ In fact, the complexation–decomplexation between *o*-QM and water is reversible and much faster than the rate of the hydration reaction. Therefore, a comparison between competitive reaction pathways has to take into consideration relative Gibbs free energies (ΔG_{TS}^\ddagger)⁴⁷ for the TSs involved in the water-assisted hydration processes (i.e., **S5out** + H₂O, **S5in** + H₂O, **S7**, **S8**, **S9**, **S10**, etc.). In particular, our attention has been focused on the competition between water dimer (through **S5** TSs) and water trimer (through **S7** TS) models, to clarify which model better describes the water-catalyzed process. Such a competition has been evaluated by relative Gibbs free energy for the **S5in** + H₂O system, with respect to **S7** TS. Although at the B3LYP/6-31G(d) level of theory the water trimer TS **S7** is slightly favored over the water dimer TS **S5in** (by 1.32 kcal mol⁻¹) in the gas phase, a proper evaluation of the hydrogen-bonding interactions with the 6-311+G(d,p) basis sets reverses such a stability order. In fact, with the inclusion of diffuse and polarization functions, **S5in** becomes 1.28 kcal mol⁻¹ more stable than **S7** in the gas phase. The inclusion of solvent effects by the C-PCM model as a single-point calculation on the gas-phase optimized geometries [at the B3LYP-C-PCM/6-311+G(d,p)//B3LYP/6-311+G(d,p) level] introduces a further and important stabilization of **S5in** in comparison to **S7**, the former being 6.82 kcal mol⁻¹ more stable than the latter in water. The above results suggest that the model used by us, which features only one water molecule directly involved in the proton transfer in a cyclic TS, is the simplest, but at the same time complete and absolutely adequate in describing the *o*-QM water-assisted alkylation process in water. The evidence that the water dimer model is also competitive in the gas phase is a remarkable observation. Therefore, even if formally the water trimer (through **S7** TS) is fit for the present reaction, water dimer (through **S5** TS) seems to be a better reactant. A favoring factor of the latter model could be, as suggested by a reviewer, that “along the reaction coordinate *o*-QM accumulates the π electronic density on the carbonyl oxygen preferentially in the out-of-plane π space and not in the in-plane lone-pair”. Concerning the water-assisted ammonia alkylation involving two additional water molecules, we failed in locating a TS like **S7**. All the TS models were transformed (during the optimization procedure) into **S4**-like TSs with an additional outer water molecule. Actually, we have been able to locate several TSs; among them, **S11** is the most stable, and it is very similar to **S9** TS.



The reaction coordinate vector of **S11** shows that the second water molecule (D) does not take part in the proton shuttle process, and that the oxygen atom of the water molecule acting as proton donor is out of the *o*-QM plane.

the polar protic solvent. We decided first to examine an explicit water molecule, to elucidate the water H-bonding effect on the reaction mechanism and on the reactivity of *o*-QM as alkylating agent,⁴⁰ and second to study the effect of the solvent bulk. We achieved the first goal by locating all the stationary points on the potential energy surfaces governing the hydration reaction (intermediate **I5**, TSs **S5in** and **S5out**) and the alkylation reactions of both ammonia (intermediate **I4**, TS **S4**) and hydrogen sulfide (intermediate **I6**, TSs **S6in** and **S6out**) in the presence of a specific water molecule complexed to the *o*-QM oxygen atom by H-bonding (see Figure 2). Such a water molecule transfers a proton (H₈) to the *o*-QM oxygen atom (O₁) and accepts another proton (H₆) from the nucleophile in a cascade process (see Figure 2 for numbering).⁴¹ Thus, the proton-transfer process does not occur, as in the absence of water, directly from the nucleophile. The water molecule, in the above "water-assisted" nucleophilic additions, acting as a proton shuttle, modifies the TS geometries, as one can see in Figure 2. The presence of a discrete water molecule allows the reactive system to reach a more perpendicular approach of the nucleophiles to the *o*-QM exocyclic methylene group. At the same time, it reduces the out-of-plane distortion of the O₁C₂C₃C₄ dihedral angle, which passes from ~14° in **S1–S3** to less than ~8° in **S4–S6**. The more favorable geometry of the nucleophile attack (from a stereoelectronic standpoint) and the lessening of the torsional strain induced by water (in the cyclic TSs) are important factors in lowering the activation barrier of the alkylation processes. In fact, on the basis of potential energies, water-assisted alkylation of ammonia, water, and hydrogen sulfide (TSs **S4**, **S5**, and **S6**) is favored by at least 12.9, 10.5, and 6.0 kcal mol⁻¹, respectively, over the same reaction without a water molecule complexed to *o*-QM (TSs **S1**, **S2**, and **S3**).⁴²

A comparison between geometric features of prereaction complexes (**I4–I6**) and related TSs (**S4–S6**) unravels other interesting aspects of the water-assisted nucleophilic addition, such as the systematic shortening of the O₁-H₈ bond length between the water molecule and the *o*-QM oxygen atom passing from the former [**I4** (1.82 Å), **I5** (1.82 Å), and **I6** (1.83 Å)] to the latter [**S4** (1.68 Å), **S5in** (1.48 Å), **S5out** (1.43 Å), **S6in** (1.44 Å), and **S6out** (1.43 Å)]. Such bond shortening is geometrical evidence of stronger H-bonding in the TSs (**S4–S6**) than in the corresponding complexes (**I4–I6**). Consistent with such bond shortening, the unscaled stretching frequencies involving the H atom being transferred in **S4** ($\nu_{\text{OH}} = 3331$ cm⁻¹), **S5in** ($\nu_{\text{OH}} = 2592$ cm⁻¹), **S5out** ($\nu_{\text{OH}} = 2331$ cm⁻¹), **S6in** ($\nu_{\text{OH}} = 2358$ cm⁻¹), and **S6out** ($\nu_{\text{OH}} = 2278$ cm⁻¹) are much lower than those of complexes **I1** ($\nu_{\text{OH}} = 3641$ cm⁻¹), **I4** ($\nu_{\text{OH}} = 3566$ cm⁻¹), **I5** ($\nu_{\text{OH}} = 3631$ cm⁻¹), and **I6** ($\nu_{\text{OH}} = 3606$ cm⁻¹).

(41) We located another type of TSs which are involved in an alternative water-catalyzed alkylation process. In these TSs, the water molecule that acts as catalyst is complexed to the *o*-QM oxygen atom, but it does not get involved in the proton-transfer process from the nucleophile to *o*-QM. These TSs show geometries very similar to the uncatalyzed alkylation processes (**S1–S3**), but their potential activation energies are always significantly higher (by ~6 kcal mol⁻¹) than those of TSs **S4–S6** where the water molecule is directly involved in the proton-transfer process.

(42) Calculated energy gaps between unassisted and water-catalyzed mechanisms are slightly wider at the B3LYP/6-311+G(d,p) level (14.4, 13.8, and 8.1 kcal mol⁻¹ for NH₃, H₂O, and H₂S, respectively) and even bigger with the smallest basis set used, 6-31G(d) (16.6, 15.9, and 11.7 kcal mol⁻¹ for NH₃, H₂O, and H₂S, respectively). The above trend is expected, since it is well known that the use of small basis sets systematically overestimates the extent of H-bonding and stabilizes significantly those structures characterized by a more extensive H-bonding network. Thus, this trend in the activation energy, as a function of the basis set, is an indirect evidence that also H-bonding plays a role among the electronic and steric effects mentioned above in lowering the activation barriers.

Thus, both geometric and spectroscopic computed properties of these stationary points demonstrate that H-bonding is stronger in TSs (**S**) than in the corresponding prereaction clusters (**I**), bringing additional stabilization to the former in comparison to the latter.

Activation potential energies suggest that a water molecule (in the gas phase or in a medium with a low dielectric constant) acts as a catalyst in the proton migration from the nucleophile to the carbonyl oxygen of *o*-QM and contributes to the lowering of the activation barrier of the alkylation reactions. The water activation is much more efficient for NH₃ and H₂O reactions than for the H₂S reaction. This gives rise, in the gas phase, to a reversal in relative activation energies of the hydration as compared to the case for hydrogen sulfide alkylation (see Table 1).

We have discussed the alkylation reaction mechanism on the basis of activation potential energies until now. Nevertheless, one must keep in mind that a proper comparison between computational and experimental results or between competing reaction mechanisms cannot neglect the entropic effects. The inclusion of non-potential-energy terms allows a direct evaluation, on the same foot, of the uncatalyzed and water-catalyzed alkylation mechanisms, because the former is selectively and strongly favored by entropic factors with respect to its assisted counterpart. Activation Gibbs free energies (ΔG^\ddagger) [computed at the B3LYP/6-311+G(d,p) level] are listed in Table 2, while a comprehensive graphical representation of the energetics of both reaction mechanisms with ammonia, water, and hydrogen sulfide are reported in Figures 4, 5, and 6, respectively. It should be emphasized, at this point, that such an approach is a novelty in the current literature; in fact, previous computational investigations on Michael additions^{25–28} neglected the entropic factors.

On the basis of ΔG^\ddagger , water-assisted alkylation of ammonia and water in the gas phase remains favored by 5.6 and 4.0 kcal mol⁻¹, respectively, over the corresponding reaction without explicit water molecule (see top half of Figures 4 and 5). In contrast, ΔG^\ddagger data of the hydrogen sulfide alkylation reaction in the gas phase suggest that such a substrate shows a slight preference for a direct alkylation without water assistance (see top half of Figure 6), even though the free energy difference ($\Delta\Delta G^\ddagger$) between the two reaction mechanisms is very small (0.8 kcal mol⁻¹ at B3LYP/6-311+G(d,p) and 1.0 kcal mol⁻¹ at the B3LYP/6-311+G(d,p),S(2df) level of theory).

As mentioned at the beginning of this section, the proton-transfer process in the water-assisted alkylation mechanism does not occur directly from the nucleophile to the *o*-QM oxygen atom but is "carried" by a water molecule which acts as a proton donor/acceptor molecule. Thus, the question arises whether the nucleophilic vs electrophilic character of the attack to *o*-QM changes on passing from the unassisted process to the water-catalyzed mechanism. The most significant contribution to the transition eigenvector of the **S4** Hessian matrix comes only from the C₄-N₅ internal coordinate (see Figure 2 for numbering). Neither N₅-H₆ nor water O₇-H₈ stretching modes make any contribution. This finding is noteworthy because it contrasts with the results obtained by Weinstein et al. regarding the water-activated alkylation of ammonia by acrolein,²⁸ where deprotonation of both ammonia and water dominates the reaction coordinate eigenvector, with negligible contribution of the C-N internal coordinate. The above discrepancy provides clear evidence that *o*-QM reactivity cannot be inferred from theoretical data on classical activated double bonds, and QMs should be considered a class of alkylating agents on its own. An

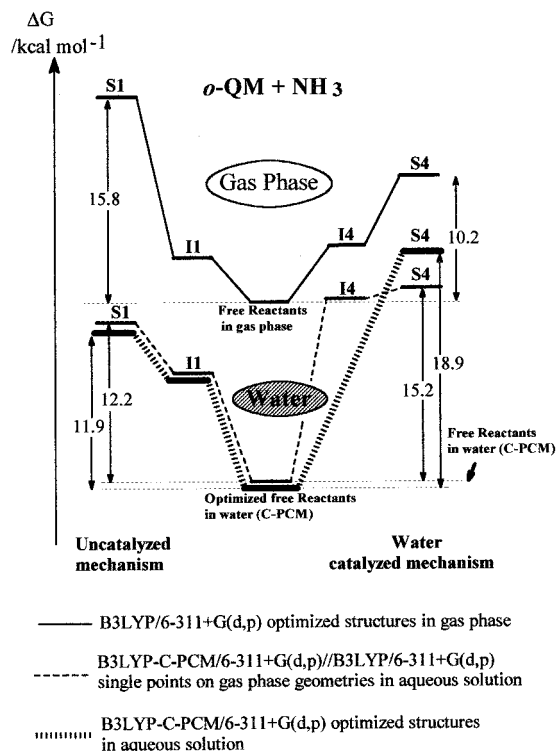


Figure 4. Free energy profiles for ammonia alkylation reaction by *o*-QM in the gas phase (continuous line), water-catalyzed (top right) and uncatalyzed (top left), and in aqueous solution by single-point calculation on the gas-phase geometries [B3LYP-C-PCM/6-311+G(d,p)/B3LYP/6-311+G(d,p)] (- - -), and optimizing both reagents and TSs in solvent [B3LYP-C-PCM/6-311+G(d,p)] (||||).

opposite behavior was identified for the **S6** reaction coordinate vector matrix, where both S_5-H_6 and water O_7-H_8 internal coordinates are the major components, while the C_4-S_5 internal coordinate makes no significant contribution. The hydration reaction assisted by water shows intermediate features: all of the three stretching modes C_4-O_5 , O_5-H_6 , and O_7-H_8 in both **S5in** and **S5out** make an important contribution to the reaction-coordinate vectors.

One may conclude that water catalysis does not affect the nucleophilic vs electrophilic behavior of the reactants in the water-assisted alkylations, since similar trends were found for catalyzed and uncatalyzed alkylation reactions. Ammonia, water, and hydrogen sulfide attack the water-complexed *o*-QM (**I2**) through TSs in which they exhibit dominant nucleophilic, nucleophilic assisted by H-bonding, and electrophilic character, respectively. Generalizing, the enhancement of *o*-QM reactivity as alkylating agent (in the gas phase) due to water catalysis parallels the nucleophilic character of the attacking reactant, which increases in the series $H_2S < H_2O < NH_3$, as demonstrated by the TS characteristics commented on above.

The relative reactivity of the three nucleophiles toward *o*-QM in the gas phase (taking into consideration both water-catalyzed and uncatalyzed reaction mechanisms), on the basis of activation Gibbs free energies (see upper parts of Figures 4–6), is as follows: $H_2S < H_2O < NH_3$. Surprisingly, hydrogen sulfide is the least reactive, in striking contrast with the experimental results,¹⁵ which clearly suggest that *o*-QM hydration is the slowest reaction. Such a discrepancy suggests that a proper computational analysis of solvent effects on *o*-QM reactivity, including bulk effects, has to be carried out.

The Role of the Electrostatic Effect of the Solvent Bulk. We have dealt so far with the effect of specific hydrogen-

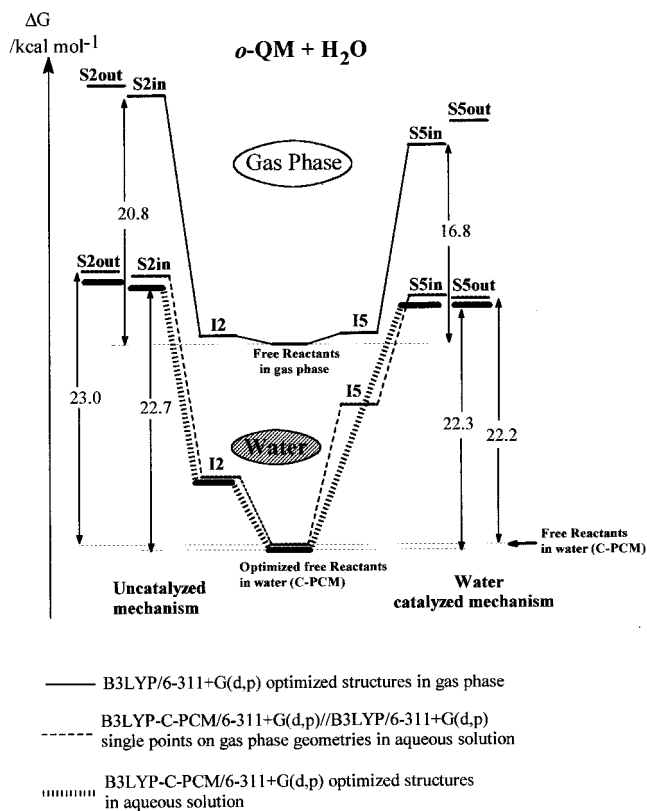


Figure 5. Free energy profiles for *o*-QM hydration reaction in the gas phase (continuous line), water-catalyzed (top right) and uncatalyzed (top left), and in aqueous solution by single-point calculation on the gas-phase geometries [B3LYP-C-PCM/6-311+G(d,p)/B3LYP/6-311+G(d,p)] (- - -) and optimizing both reagents and TSs in solvent [B3LYP-C-PCM/6-311+G(d,p)] (||||).

bonding interaction of water on the *o*-QM reactivity. Nevertheless, water is also a highly polar solvent; therefore, we cannot ignore its bulk effects. We now examine the effect of the bulk solvent reaction field on the energetics of both water-assisted and unassisted alkylation of ammonia, water, and hydrogen sulfide, to obtain a fairly good and complete reproduction of solvent effect on the activation Gibbs free energy of the alkylation reactions by *o*-QM.

(a) Bulk Effects on Unassisted Mechanism. Barone et al. showed that even important geometrical changes have little influence on the solvation energy in the addition reaction between hydrogen cyanide and methanimine.³⁸ We confirmed such a trend in our uncatalyzed reactive system, optimizing the structure of **I1–I3** intermediates and **S1**, **S2in**, and **S3in** TSs in water. The most meaningful bond lengths of these stationary points computed at the B3LYP-C-PCM/6-311+G(d,p) level are reported in Figure 1 in parentheses and bold characters. Some significant geometric differences between optimized structures in solvent and in the gas phase are evident, such as the lengthening of the forming C--Nu bonds (i.e., by 0.34 Å in the ammonia alkylation) with earlier TSs, and a more perpendicular trajectory (with respect to the *o*-QM methylene group) of the attacking nucleophiles. Nevertheless, the difference in energy between these fully optimized structures in solvent and single-point calculations on the optimized gas-phase structures never exceeds 0.5 kcal mol⁻¹ (at least for TSs without water catalysis such as **S1–S3**; see Table 2).

The free energy of solvation (δG in Table 2) is important and stabilizes TSs less than reactants, with the exception of **S1**. As a result, the bulk effect of the solvent (evaluated from

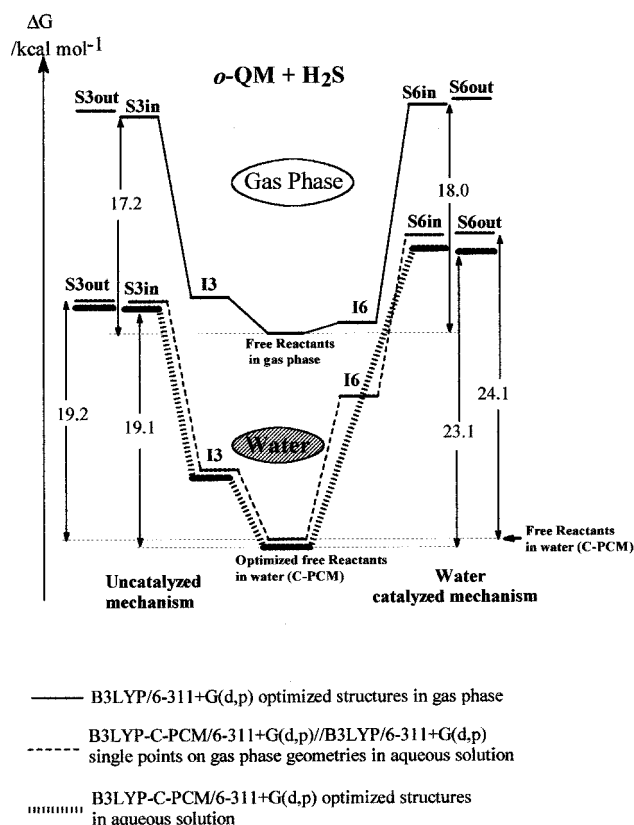


Figure 6. Free energy profiles for hydrogen sulfide alkylation reaction by *o*-QM in the gas phase (continuous line), water-catalyzed (top right) and uncatalyzed (top left), and in aqueous solution by single-point calculation on the gas-phase geometries [B3LYP/6-311+G(d,p)//B3LYP-C-PCM/6-311+G(d,p)] (---) and optimizing both reagents and TSs in solvent [B3LYP-C-PCM/6-311+G(d,p)] (···).

solvent-optimized TSs) increases the activation free energies of all “unassisted” alkylation reactions (by 1.7–1.9 kcal mol⁻¹), with the exception of the ammonia alkylation (S1), which is reduced by -3.9 kcal mol⁻¹. This exception finds a reasonable explanation in the zwitterionic nature of S1, which is the consequence of its “pure nucleophilic” reaction mechanism. In fact, S1 is the only stationary point, unassisted by water, showing a higher dipole moment (5.01 D in the gas phase; 7.41 D in bulk) than the reactants (*o*-QM, 3.60 D; H₂O, 2.16; NH₃, 1.70 D; H₂S, 1.35 in the gas phase; *o*-QM, 5.10 D; H₂O, 2.49 D; NH₃, 2.06 D; H₂S, 1.61 D in bulk). S2 (3.46, 3.42 D for S2_{in} and S2_{out}, respectively) and S3 (3.21, 3.32 D for S3_{in} and S3_{out}, respectively) TSs are less polar than S1; thus, the electrostatic solvent stabilization (see Table 3) for the former TSs is lower than the latter one.

(b) Bulk Effects on Water-Assisted Mechanism. The water bulk has a more important effect on water-assisted alkylation reactions than on the unassisted mechanism. In fact, as estimated by single-point calculations on the gas-phase optimized geometries [at the B3LYP-C-PCM/6-311+G(d,p)//B3LYP/6-311+G(d,p) level], S4, S5_{in}, S5_{out}, S6_{in}, and S6_{out} TSs are less stabilized than the corresponding free reactants by 5.0, 5.5, 2.8, 6.2, and 5.5 kcal mol⁻¹, respectively (see Table 2, $\delta\Delta G$ column). Such an effect has important consequences on the competition between the assisted and unassisted mechanisms, particularly for N-centered nucleophiles. This aspect will be discussed in more detail in the next paragraph. Thus, to produce more reliable data concerning the water-catalyzed processes in water, we further refined the solvent model for alkylation reactions, optimizing S4–S6 TSs in water at the B3LYP-C-PCM/6-

311+G(d,p) level of theory. Significant geometric differences between optimized structures in solvent and in the gas phase are evident in Figure 2, such as the lengthening of the forming C–Nu bond with earlier TSs for the alkylation of ammonia and water. Such a bond lengthening is particularly large (0.74 Å) in the water-catalyzed alkylation of ammonia (S4), but it becomes smaller (0.13 Å) in the hydration reaction (S5). The effect of the solvent bulk is opposite on TS geometries involving the water-assisted alkylation of hydrogen sulfide (S6), where the forming C–S₅ bond, in both S6_{in} and S6_{out}, is slightly shortened in solution by 0.12–0.15 Å. Despite these significant differences between TS geometries in the gas phase and in solution, ΔG_{soln} data (in Table 2) suggest that the majority of solvent effect (similar to the case in the uncatalyzed reactions) is fairly well reproduced by single-point calculations on gas-phase optimized geometries [B3LYP-C-PCM/6-311+G(d,p)//B3LYP/6-311+G(d,p) level]. There is only one important exception: the ammonia alkylation reaction catalyzed by water (S4). In fact, its activation free energy experiences a considerable increase (by 3.7 kcal mol⁻¹) on going from the value obtained by single-point calculation on S4 TS in the gas phase [15.2 kcal mol⁻¹, at the B3LYP-C-PCM/6-311+G(d,p)//B3LYP/6-311+G(d,p) level] to that obtained by full optimization of S4 TS in water [18.9 kcal mol⁻¹, at the B3LYP-C-PCM/6-311+G(d,p) level].

The Overall Solvent Effect on Alkylation Reaction Mechanisms. Comparison of the activation Gibbs free energy data, obtained from water optimized TSs and reactants (ΔG_{soln} , listed in Table 2 for TSs S1–S6), for the alkylation of the same nucleophile with and without addition of an explicit water molecule (S1 vs S4, S2 vs S5, and S3 vs S6 in Figures 4, 5, and 6, respectively) reveals an interesting and different scenario with respect to that in the gas phase. In particular, for the alkylation reaction of ammonia in the gas phase (see Figure 4), it is quite evident that the most favorable mechanism of the nucleophilic addition of NH₃ to *o*-QM is a 1,4-addition assisted by a discrete water molecule, as demonstrated by the lower energy of S4 than of S1 (by 5.6 kcal mol⁻¹, top half of Figure 4). However, in water solution, the unassisted reaction should dominate its catalyzed counterpart, going through S1 TS, which is 7.0 kcal mol⁻¹ lower in energy than S4 (bottom half of Figure 4).

In the case of the alkylation of H₂S by *o*-QM (Figure 6), the effect of the water bulk shifts the reaction toward the uncatalyzed mechanism (S3), which was already slightly favored in the gas phase on the basis of activation Gibbs free energies (by 0.8 kcal mol⁻¹, top half of Figure 6). Such a mechanism becomes dominant in water, S3 TSs being more stable than S6 TSs by 4.0 kcal mol⁻¹ (bottom half of Figure 6).

In contrast, activation induced by water complexation should still play an important role in the *o*-QM hydration reaction even in water as solvent. Water-assisted hydration (S5, in Figure 5) is clearly favored over the uncatalyzed counterpart (S2) in the gas phase by 4.0 kcal mol⁻¹ (top half of Figure 5). Such an energy gap is significantly reduced in solution, where the water-catalyzed mechanism is still slightly favored only by 0.5 kcal mol⁻¹ (bottom half of Figure 6). However, the above energy difference between the two reaction mechanisms should be slightly enlarged by the presence of the high water concentration in a water solution.⁴³ The importance of the water-catalyzed mechanism in the control of *o*-QM reactivity could likely be

(43) Taking into consideration water concentration in a water solution (55.5 M) should introduce a further stabilization (estimated in 2 kcal mol⁻¹) in favor of the water-assisted mechanisms.

generalized to other oxygen-centered nucleophiles. Note that our result makes an additional contribution to the debate on the *o*-QM hydration reaction, which still attracts considerable attention,^{15,23,44} suggesting that the hydration reaction of *o*-QM likely involves two molecules of water.

Summing up, the *o*-QM alkylation of nitrogen and sulfur nucleophiles in water solution can be reasonably well described with a simple reaction mechanism where no water is directly involved; that is, neglecting the specific interaction (H-bonding) of *o*-QM with the solvent. The *o*-QM reactivity with these nucleophiles in water solution should be well reproduced by gas-phase TSs and by considering only the water bulk effect using single-point calculations on the gas-phase geometries. Hydration reaction requires a supramolecular reaction model, with two water molecules, where both the specific and the bulk effects of water have been taken into account.

It is also noteworthy that the reactivity of ammonia is always higher than that of hydrogen sulfide and that the hydration of *o*-QM is the slowest reaction in water. Such a computed reactivity scale in water (NH_3 , $\Delta G^\ddagger = 11.9 > \text{H}_2\text{S}$, $\Delta G^\ddagger = 19.1 > \text{H}_2\text{O}$, $\Delta G^\ddagger = 22.2 \text{ kcal mol}^{-1}$) well reproduces the experimental data concerning alkylation of amines, thiols, and water in aqueous solution.¹⁵

Our results suggest a proper computational model of *o*-QM reactivity which clarifies the role of water catalysis in alkylation and hydration reactions. Therefore, the present results should be of interest to those experimentalists dealing with QM as enzymes inhibitors and cross-linking agents.

Conclusion

In this paper we have reported a computational study on the reactivity of *o*-QM as alkylating agent of nitrogen, oxygen, and sulfur nucleophiles, in the gas phase and in water, taking into consideration (in two consecutive steps) both the specific and the bulk effects of such a solvent, which often has been used by the experimentalists. The results can be summarized as follows:

In the gas phase, the alkylation of NH_3 by *o*-QM is an example of “pure nucleophilic addition” onto *o*-QM with development of a zwitterionic TS. The alkylation reaction mechanism of water can be defined as “nucleophilic addition assisted by H-bonding”, while in the alkylation of H_2S this latter exhibits a dominant electrophilic interaction with *o*-QM at the TS. Thus, along the series NH_3 , H_2O , H_2S there is a progressive shift from a “nucleophilic” interaction to an “electrophilic” one of the adding reactant with *o*-QM.

(44) Chiang, Y.; Kresge, J.; Zhu, Y. *J. Am. Chem. Soc.* **2000**, *122*, 9854.

(45) Benson, S. *Thermochemical Kinetics*; Wiley: New York, 1968; p 8.

(46) Rastelli, A.; Bagatti, M.; Gandolfi, R. *J. Am. Chem. Soc.* **1995**, *117*, 4965.

(47) Seeman, J. I. *Chem. Rev.* **1983**, *83*, 83.

Specific solvent effects, taken into account by explicit addition of a water molecule to prereaction clusters and TSs, suggest that water, in the gas phase, is directly involved in a proton-transfer process which lowers significantly both the activation potential energies (by $\sim 10\text{--}12 \text{ kcal mol}^{-1}$) and activation Gibbs free energies (by $\sim 4\text{--}5 \text{ kcal mol}^{-1}$) for the alkylation of nitrogen and oxygen nucleophiles. That is, in the gas phase the “water-catalyzed” processes should dominate their “uncatalyzed” counterparts. Hydrogen sulfide alkylation in the gas phase does not benefit such a water activation, since the uncatalyzed mechanism is slightly favored over the catalyzed one (by roughly 1 kcal mol^{-1}).

Bulk solvent effects of water, described by the C-PCM model, significantly modify the relative importance of the uncatalyzed and water-assisted alkylation mechanisms of *o*-QM in comparison to the case in the gas phase. Surprisingly, the uncatalyzed mechanism becomes highly favored over the catalyzed one in the alkylation reaction of ammonia and hydrogen sulfide. *This remarkable observation should allow study of the alkylation processes of more complex nitrogen and sulfur biological nucleophiles (such as nucleobases, chain NH_2 peptides, or glutathione-containing peptides) by *o*-QMs, with a simple reaction model which neglects the specific effects of water and computes *o*-QM reactivity in solution, taking into account only the bulk effects of the solvent.* Work is still in progress in our group in order to address the problem of QMs selectivity as alkylating agents and to generalize the conclusion obtained with ammonia also to real biological N-centered nucleophiles (such as nucleobases).

However, the above reaction model, which neglects the specific effect of the solvent, cannot be applied to the *o*-QM hydration reaction and, likely, to the alkylation of less reactive oxygen-centered nucleophiles in water. A proper computational model describing the QMs reactivity in such reactions requires consideration of both specific and bulk solvent effects.

Acknowledgment. Financial support from Pavia University (“Fondo Giovani Ricercatori 1999”) is gratefully acknowledged. We also thank CICAIA (Modena University) for computer facilities and Prof. Remo Gandolfi for useful discussions.

Supporting Information Available: Electronic energies, Cartesian coordinates of stationary points in Figures 1 and 2, in the gas phase, optimized at the B3LYP/6-311+G(d,p) and B3LYP/AUG-cc-pVTZ levels, and geometries optimized in solvent (water) at the B3LYP-C-PCM/6-311+G(d,p) level of theory (PDF). This material is available free of charge via Internet at <http://pubs.acs.org>.

JA010433H